A New Echelle Grating... for EFOSC!

As this issue of the Messenger goes to press, we start analysing the results of some successful test observations with a new transmission echelle mounted on EFOSC. In combination with two different cross-dispersers it provides echelle spectra in two standard formats: the first covering the spectral region from 3700 to 7400 Å, the second from 5400 to 10000 Å.

From a first rough estimate the limiting magnitude in the continuum is about 18. (S/N ≃ 20), the resolving power with a 1 arcsecond slit 2,300. This grating should satisfy both EFOSC users who have longed for a resolution higher than the one presently available and those CASPEC fans who want to work on fainter objects, even at a loss of resolution. In combination with broad-band filters, it gives also the possibility to do long slit work on extended objects.

The reduction of the test observations requires some modification in the MIDAS Echelle reduction package and will take a few weeks.

Some minor mechanical modifications to the instrument are also necessary.

We will make an effort to make this new option available to EFOSC users from the start of period 38.

A New Camera and a CCD Detector for the Coudé Echelle Spectrograph

H. DEKKER, B. DELABRE, S. D'ODORICO, H. LINDGREN, F. MAASWINKEL, R. REISS, ESO

The concept of a new, faster camera for the CES originated in 1981, when it was pointed out that because of the narrow wavelength band covered at one time by the CES, the required correction for chromatic dispersion would be rather small. A dioptric design was worked out at ESO and the optics were manufactured by Carl Zeiss, FRG. F. Maaswinkel tested the optical quality in Garching and installed the camera at La Silla in November 1985.

At the same time a new CCD Camera was installed at the CES. It mounts a double density RCA CCD (ESO CCD # 8, 640 × 1,024 pixels, 15 μm square). The characteristics of the camera, of the CCD and the first astronomical results are discussed below. At comparable resolution, a gain of at least 2 magnitudes is achieved with respect to the Long Camera with the reticon detector.

1. Design and Optical Properties of the New "Short" Camera

The design of the Short Camera is shown in Figure 1. The camera consists of 5 lenses, mounted in a tube; the last lens is moved by a focusing motor to correct for the chromatic dispersion. The cryostat is coupled to the camera with a field lens in front of the vacuum window. The focal length of the camera is 516 mm (at 632.8 nm), its effective aperture is f/2.58. The corrected field at the detector is 30 mm, therefore in principle also a reticon can be used. The transmission as measured at ESO is shown in Figure 2. Comparing it with the

Long Camera, which has an average transmission of 65%, one sees that for the useful range the new Camera performs better.

The camera has been tested extensively in the optical laboratory. Using red light and the Twyman-Green interferometer it showed a quality of 0.7 λ (on axis) and 1.2 λ (field position 12 mm); by scanning the image of a pinhole over the detector the point spread function of the camera was derived. This gave an energy concentration of 80% within 8 μm (on axis) at 480 nm. From these two measurements one expects that the energy concentration of the camera + CES will be 80% within a 15 μm pixel for the total wavelength range (360–1,100 nm): This conclusion agrees with the original computations of image quality. In tests with a position-sensitive detector it was verified that upon moving the focusing lens a point image did not suffer a lateral shift larger than ± 3 μm.

2. The Operation of the New Camera and of the CCD at the CES

To facilitate the operation of the CCD detector and the switching between Short and Long (Maksutov) cameras, and also to bring the CES instrumentation programme in accordance with those at other instruments (EFOSC, CASPEC), the control programme of the CES had been rewritten by E. Allaert. In the new programme the user can select the camera of his choice by softkeys (assuming that it has been mounted!). The only difference the user "sees", is in case of the Short Camera the display of the two-dimensional CCD picture on the Ramtek screen. In the instrumentation programme a focusing curve for the Short Camera is included, which should not be changed if the camera + CCD are not disassembled between observation runs. One nice feature of this curve is that during future maintenance of the instrument one easily could introduce
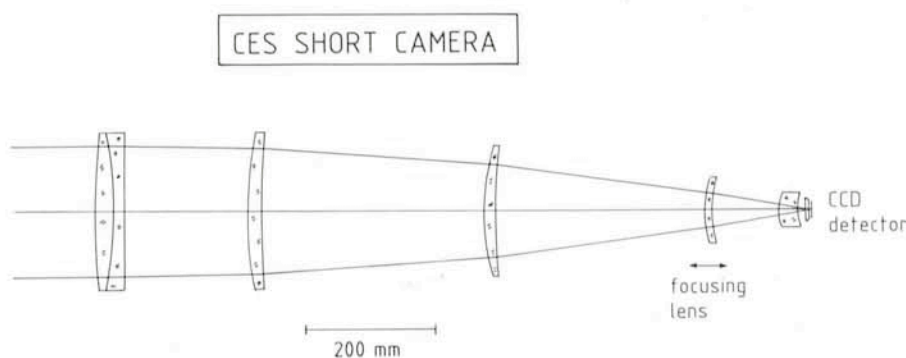

CES SHORT CAMERA

CCD detector

focusing lens
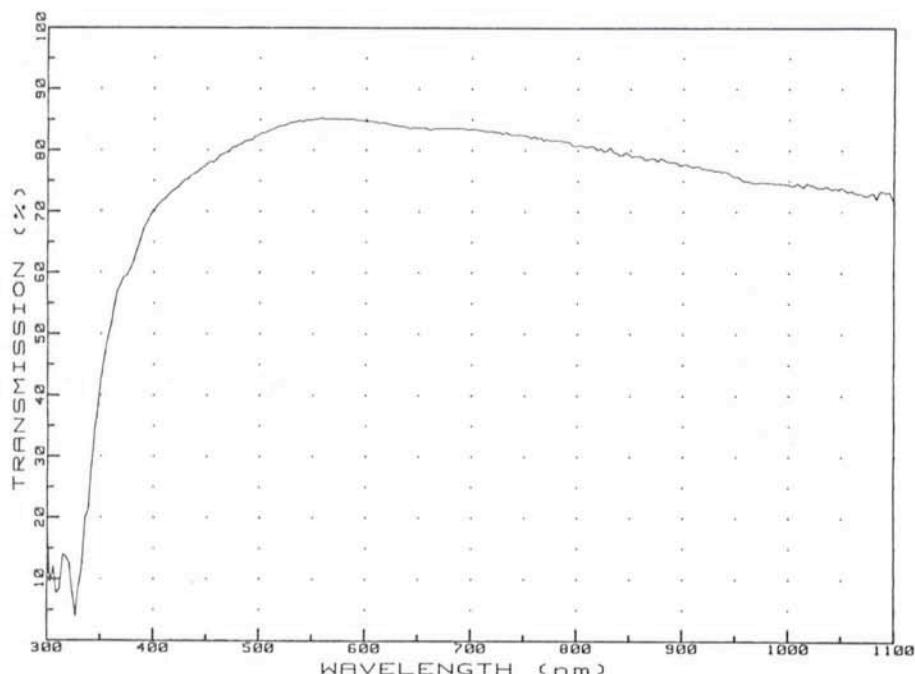
200 mm

Figure 1: *The optical layout of the new camera.*

Figure 2: *Transmission curve of the new camera.*

was measured by observations of standard stars with a widely open slit. Table 2 summarizes the results at three different wavelengths. The expected S/N ratio for a given star can be computed from these values once allowances are made for extinction, slit losses, actual dispersion and the read-out noise of the CCD. The characteristic intensity variations due to interference within the silicon layer of the CCD (fringes) are visible in this chip at wavelengths longer than about 5500 Å with an amplitude of less than 10 %. They are well corrected by flat field.

In the reduced spectra of bright stars, where the read-out noise is negligible with respect to the photon noise, S/N ratios of 250 have been measured. It is likely that the values can be further improved by co-adding several exposures and taking special care in the reduction phase.

The resolution of the CES with this camera has been estimated in two different ways. From the FWHM of the Thorium lamp lines observed with a 240 µm wide slit (1.1 arcsecond) and fitted with a Gaussian one derives a resolving power of 72,000 from 3900 to

offset steps if this would be necessary. At the installation run the CES was changed from the blue to the red path and back within a few minutes, so this operation with the Short Camera does not cause any delay for the observer. The change-over to the Long Camera should also be a rather simple procedure: the cameras are fixed on support tables, which can be mounted on the 3 point pillar support in the CES room.

In the last years, the most commonly used detector at the CES has been a reticon array of 1,872 diodes (15 × 700 µm in size). With the Short Camera we have installed a new detector, a double density RCA CCD, whose characteristics are summarized in Table 1 and Figure 3.

The advantages of the CCD with respect to the reticon are the much lower r.o.n., the two-dimensional capability and a higher quantum efficiency below 6000 Å. The main advantage of the reticon is the larger linear size. In the direction of the dispersion, the pixel size is identical. Two pixels in the dispersion direction on the detector correspond to about 2″0 and 1″6 in the focal plane of the telescope, in the dispersion direction and perpendicular to it respectively. The observers can bin the CCD in the direction perpendicular to the dispersion at no loss of resolution when the seeing is poor.

The number of pixels in this CCD is such that the reading time and the volume of the data which are accumulated are not negligible. To save both time and space, the observers can preselect a strip in the CCD which contains both the spectrum and sufficient background for the data reduction and recover only those data at the end of the exposure.

3. Efficiency, Resolution and First Astronomical Results

The efficiency of the telescope + CES + Short Camera + CCD combination

TABLE 1: *Properties of ESO CCD # 8*

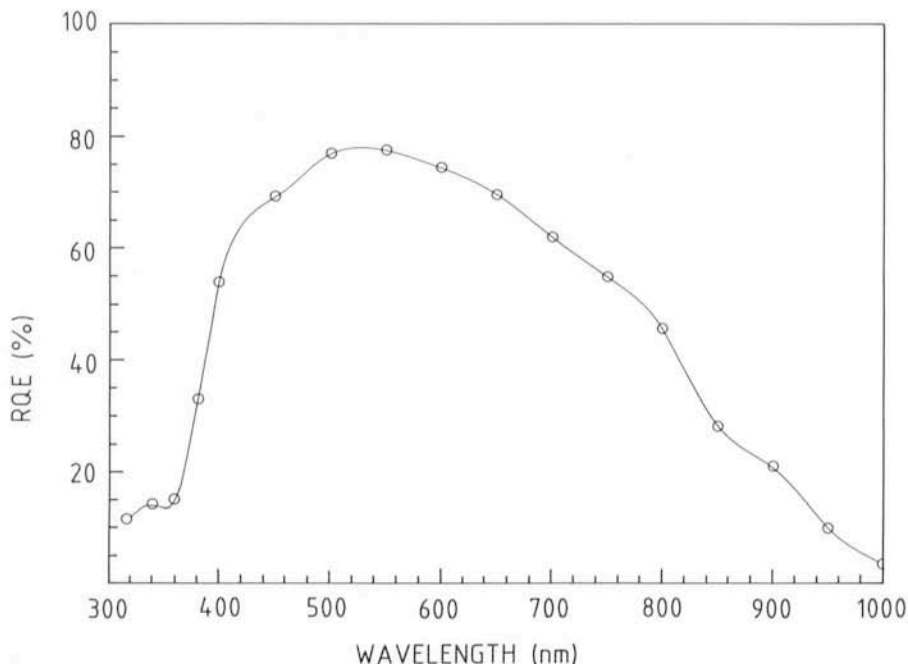| Chip type	RCA thinned backside illuminated – S. No. 5103/2/6
Telescope	Normally used at the CAT 1.4 m
Format	640 × 1,024 pixels, 15 µm × 15 µm
e-/ADU and gain	6 e-/ADU at G 50
r.o.n.	36 e-
Quantum efficiency	See Figure 3
Dark current	60 e-/pixel/hour at 140°
Blemishes	Dead column at x = 41. Several column pairs with small negative/positive offsets

Figure 3: *Quantum efficiency of the ESO CCD # 8.*

TABLE 2: *Reciprocal Dispersion and Efficiency*

Wavelength (Å)	Å/mm	m^*_λ
3930	2	14.4
5000	2.7	15.4
5890	3.2	15

Magnitude per unit frequency of a star for which 1 photon/s/Å is recorded. Data are relative to a 5 arcsecond wide slit and are corrected for extinction.
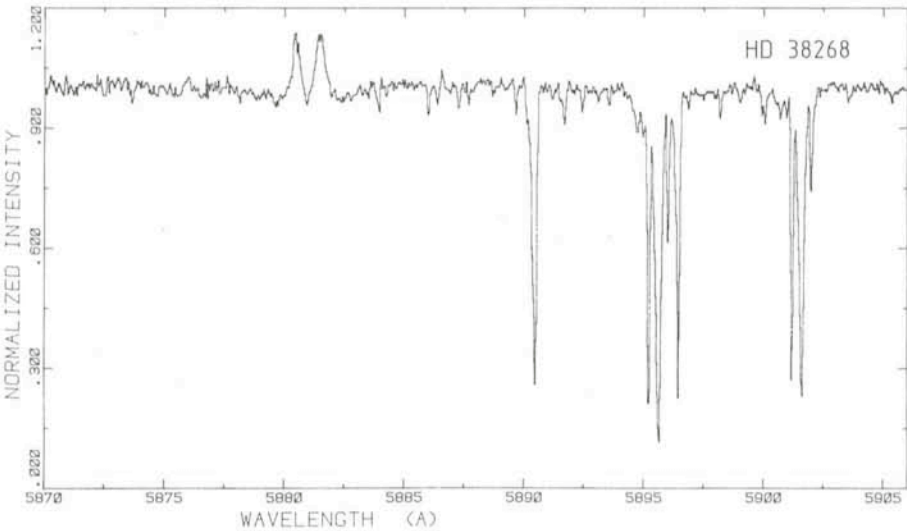

Figure 4: *A spectrum of the central object of the 30 Dor nebula in the LMC (HD 38268 = Radcliffe 136) centred at 5890 Å. It is the average of two 1-hour exposures. The slit was 1.1 arcsecond wide. The resolving power, as measured from the FWHM of the comparison lines, is 72,000 and the S/N ratio in the continuum about 100. The quality of this spectrum obtained with a 1.4-m telescope clearly surpasses that of similar observations with larger apertures reported in the literature. Apart from the interstellar Na I absorptions by gas in the galaxy and in the cloud, two emission components of the He I nebula line and a number of telluric absorptions are also seen.*
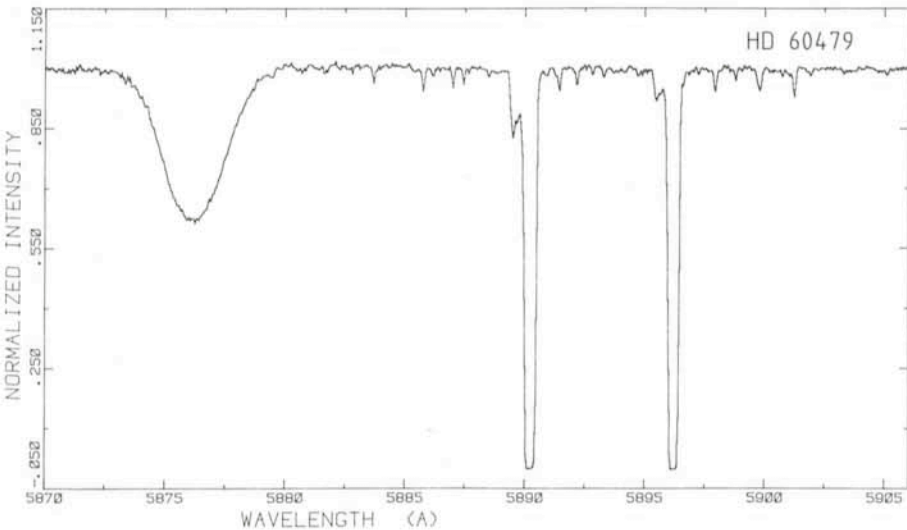

Figure 5: *A spectrum of the early type (09.5 Ib) star HD 60479 centred on the interstellar sodium D_1 and D_2 lines. The star is heavily reddened with a V magnitude of 8.41 and B-V colour +0.34. The exposure time was 90 minutes. Also seen is the stellar line from He I at 5876 Å. Resolving power is 72,000 and the S/N in the continuum about 250. The faintest absorption lines seen in the spectrum (mostly telluric absorptions) have equivalent widths of 5 mÅ.*

TABLE 3: *Heliocentric Velocities (km/s) of Interstellar Na I Lines in R 136*

Component	Gal	1	2	3	4	5
D_2	22.5	241.1	252.6	265.7	286.2	306.6
D_1	24.2	241.4	258.	267.1	287.8	308.1

6000 Å. Another estimate has been based on the analysis of a solar spectrum centred at 5170 Å. In this wavelength region the spectrum has some closely spaced doublets (5167.4 Å, 5168.9 Å, 5177.3 Å, 5188.7 Å). We assigned a "spatial" frequency to these doublets (assuming the modulations to be sine waves); by comparing the measured modulation depths with the highly resolved data from the Liège solar atlas, we could infer a Modulation Transfer Function (MTF) for the whole instrument. As a criterion for the limiting resolution, the maximum frequency where MTF = 0.2 was taken (1). In our case a limiting frequency of 14−16 line pairs/Å was obtained. This again would correspond to a resolution of 70,000−80,000.

We present in Figures 4 and 5 two reduced spectra from the test run with the instrument to give future users a feeling of its performance.

Figure 4 shows the spectrum of the central object of the 30 DOR nebula in the LMC centred at λ = 5890 Å. The quality compares rather well with that of observations at similar resolution but with larger telescopes (2, 3). In this spectrum the complex structure of the interstellar absorption lines of Na I is of great interest. The heliocentric velocities of the different components are listed in Table 3. Thanks to the high S/N which has been achieved we discover two new faint components at v = 241.2 and 258 km/sec (the first having been measured in Ca II in the works quoted above). We also measure two emission components of He I at v = 232.7 and 298.5, that is symmetrical with respect to one of the absorption lines. From the measurements on the telluric lines, we estimate the velocity accuracy to be better than 2 km/sec. The agreement with the values from other authors is quite good. A detailed discussion of these data is outside the purpose of this article, but they clearly demonstrate that quite useful results can be obtained with the new camera and detector.

References

1. D. Enard, *ESO Technical Report* No. 10.
2. J.C. Blades, 1979, *M.N.R.A.S.,* **190**, 33.
3. N.R. Walborn, 1980, *Ap. J.* **235**, L 101.

Acknowledgements